

# Bio-inspired green synthesis of Fe<sub>3</sub>O<sub>4</sub> magnetic nanoparticles using watermelon rinds and their catalytic activity

Ch. Prasad<sup>1</sup> · S. Gangadhara<sup>1</sup> · P. Venkateswarlu<sup>1</sup>

Received: 4 January 2015 / Accepted: 18 July 2015 / Published online: 21 August 2015  
© The Author(s) 2015. This article is published with open access at Springerlink.com

**Abstract** Novel and bio-inspired magnetic nanoparticles were synthesized using watermelon rinds (WR) which are nontoxic and biodegradable. Watermelon rind extract was used as a solvent and capping and reducing agent in the synthesis. The Fe<sub>3</sub>O<sub>4</sub> MNPs were characterized by using transmission electron microscopy (TEM), X-ray diffraction (XRD), Fourier transform infrared spectroscopy (FTIR) and vibrating sample magnetometer techniques (VSM). XRD studies revealed a high degree of crystalline and monophasic Fe nanoparticles of face-centered cubic structure. FTIR analysis proved that particles are reduced and stabilized in solution by the capping agent that is likely to be proteins secreted by the biomass. The present process is an excellent candidate for the synthesis of iron nanoparticles that is simple, easy to execute, pollutant free and inexpensive. A practical and convenient method for the synthesis of highly stable and small-sized iron nanoparticles with a narrow distribution from 2 to 20 nm is reported. Also, the MNPs present in higher saturation magnetization (Ms) of 14.2 emu/g demonstrate tremendous magnetic response behavior. However, the synthesized iron nanoparticles were used as a catalyst for the preparation of biologically interesting 2-oxo-1,2,3,4-tetrahydropyrimidine derivatives in high yields. These results exhibited that the synthesized Fe<sub>3</sub>O<sub>4</sub> MNPs could be used as a catalyst in organic synthesis.

**Keywords** X-ray diffraction · Fe<sub>3</sub>O<sub>4</sub> MNPs · TEM · VSM · Catalyst activity

## Introduction

In recent years, nanostructured materials have attracted great interest owing to their particular physical and chemical properties (Zhou et al. 2005). Generally magnetic iron oxide nanoparticles are utilized as gas sensors and pigments, recording material and electrophotographic developer, such as in magnetic resonance imaging (MRI) (Chen et al. 2010, 2011), in lithium ion battery field (Sanchez et al. 2012), as optical material (Hornbaker et al. 2002), in catalysis (Lu and Schmidt 2004), environmental remediation (Zhang et al. 2012; Cheng et al. 2012), tissue-repair engineering (Gupta and Gupta 2005) and targeted drug delivery (Jabera and Mohsen 2013; Sun et al. 2008; He et al. 2012), biomedical treatment and in spintronic devices (Wang et al. 2007; Zou et al. 2005; Hayakawa et al. 2007; Durmus et al. 2009). Large varieties of methods have been reported in the literature for the synthesis of Fe<sub>3</sub>O<sub>4</sub> MNPs such as hydrothermal process (Hua and HeQing 2008), sonochemical method (Nazrul Islam et al. 2011), micro-emulsion technique (Deng et al. 2003), electrochemical route (Franger et al. 2004) and co-precipitation method (Wu et al. 2008). The green synthesis of nanoparticles has been proposed as a cost-effective environmental-friendly and an alternative to chemical and physical methods. The literature survey reveals that some of the reports are available on green synthesis of Fe<sub>3</sub>O<sub>4</sub> MNPs (Cai et al. 2010; Lu et al. 2010; Venkateswarlu et al. 2013, Wang et al. 2009). Extensive literature reports reveal that the use of naturally available fruit waste material has not been investigated for the synthesis of Fe<sub>3</sub>O<sub>4</sub> MNPs.

✉ P. Venkateswarlu  
ponneri.venkateswarlu@gmail.com

<sup>1</sup> Biopolymers and Thermophysical Laboratories, Department of Chemistry, Sri Venkateswara University, Tirupati 517 502, Andhra Pradesh, India

Hence, in the present study, naturally abundant watermelon rinds were used for the synthesis of  $\text{Fe}_3\text{O}_4$  MNPs by the green route. Watermelon (*Citrullus lanatus*), being the heaviest and largest fruit, is one of the cheapest and most abundant available in India with 3 lakh tons produced every year. The red flesh of watermelon present inside is sweet, ripe and used for juices and salads, but the outer rind is considered as waste and has no commercial value. Watermelon rind (WR) consists of cellulose, citrulline, pectin, proteins and carotenoids (Lakshmipathy and Vinod 2013; Li and Yan 2012; Narayanan and Sakthivel 2011) which are rich in hydroxyl (cellulose) and carboxylic (pectin) functional groups. In this paper, for the first time, watermelon rind powder extract (WRPE) was used as capping or reducing agent for synthesis of  $\text{Fe}_3\text{O}_4$  MNPs. However in this paper, a facile completely green synthesis of  $\text{Fe}_3\text{O}_4$  MNPs has been developed using watermelon rind extract. Further, the synthesized  $\text{Fe}_3\text{O}_4$  nanoparticles were used as a catalyst for the preparation of biologically interesting ethyl 6-methyl-4-(4-nitrophenyl)-2-oxo-1,2,3,4-tetrahydropyrimidine-5-carboxylate.

## Materials and methods

### Materials

All the chemicals were of analytical reagent grade and used without further purification. Doubly distilled water was used in all the synthesis procedures. Ferric chloride hexahydrate ( $\text{FeCl}_3 \cdot 6\text{H}_2\text{O}$ ), ethyl acetoacetate, aldehyde, ethanol, urea and sodium acetate were purchased from Sigma Aldrich.

### Preparation of the extract

The watermelon rinds were thoroughly rinsed with double distilled water to remove the fine dust particles and, later, dried under shade at room temperature for 24 h under dust-free condition. The dried watermelon rinds were ground with a mortar and pestle to make a powder. An amount of 10 g of rind powder was mixed with 100 mL double distilled water and refluxed for 2 h at 80 °C, until the color of the aqueous extract solution changed from watery to pale yellow. The resultant composition was cooled to room temperature and filtered with a Whatman no. 1 filter paper and the final extract was stored at  $-4$  °C for further use.

### Synthesis of $\text{Fe}_3\text{O}_4$ MNPs

$\text{Fe}_3\text{O}_4$  MNPs are prepared through an easy and eco-friendly method. In a conventional reaction procedure, 2.26 g of  $\text{FeCl}_3 \cdot 6\text{H}_2\text{O}$  and 6.46 g of sodium acetate are dissolved in

30 mL of freshly prepared watermelon rind powder extract (WRPE) and stirred vigorously for 3 h at 80 °C. The resulting solution becomes homogenous black in color after 3 h showing the formation of  $\text{Fe}_3\text{O}_4$  MNPs solution. The resulting solution is cooled to room temperature and the attained black product is isolated by applying an external magnetic field and washed with ethanol and dried in a vacuum oven at 90 °C for 12 h and kept in a stoppered bottle for further use.

### General procedure for the synthesis of compounds

$\text{Fe}_3\text{O}_4$  nanoparticles (5 mmol) were added to a mixture of ethyl acetoacetate (1, 1.0 mmol), aldehyde (2, 1.2 mmol) and urea (3, 1.2 mmol) in ethanol (5.0 mL). The reaction mixture was heated under reflux for 10–12 h. After the reaction was completed, as indicated by TLC, the solvent was removed in a reduced pressure evaporator. The residue was purified by column chromatography on silica gel to afford the final product.

### Characterization

The synthesized nanoparticles are characterized by X-ray diffractometer Seifert 3003 TT with  $\text{Cu-K}\alpha$  radiation having a wavelength of 1.52 Å. Morphological and size distribution was done with transmission electron microscope (TEM) images; selected area electron diffraction (SAED) patterns and high-resolution TEM (HRTEM) images were obtained on JEM-2100 with an accelerating voltage of 200 kV system of JEOL. The magnetic measurement was recorded at room temperature (300 K) using a vibrating sample magnetometer (VSM, LKSM-7410). FTIR measurements of watermelon rind extract and prepared sample were made with Thermo Nicolet FTIR -200 Thermo Electron Corporation.

## Results and discussion

### FTIR characterization

FTIR analysis is used for characterizing the synthesized  $\text{Fe}_3\text{O}_4$  MNPs. Moreover, the existence of surface functional groups in metal interactions is because the watermelon rinds are rich in polyphenols, acid derivatives and proteins. Figure 1a indicates the FTIR spectra of watermelon rind extract and the watermelon rind extract of iron nanoparticles, curve 1b. The two curves showed that there was a variation in the intensity of bands in different regions. A major peak was identified at  $3635\text{ cm}^{-1}$  corresponding to the O–H stretching vibrations (polyphenolic group). This peak shifted from  $3625$  to  $3340\text{ cm}^{-1}$ ,

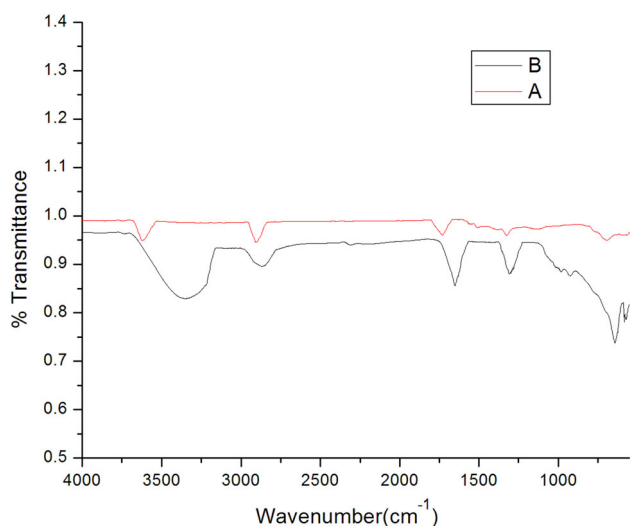


**Fig. 1** FTIR spectrum of the **a** WR extract and **b** synthesized  $\text{Fe}_3\text{O}_4$  MNPs

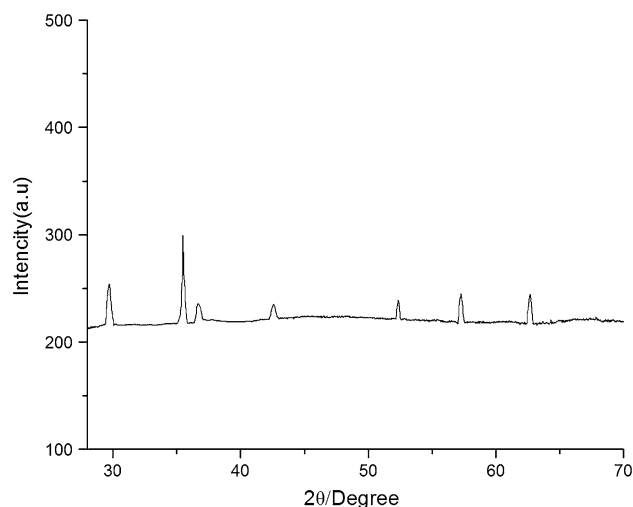
indicating the involvement of polyphenols in the synthesis of iron nanoparticles. The peak shift from  $2910$  to  $2855\text{ cm}^{-1}$  is assigned to the C–H stretching vibration of the methyl and methoxy groups, respectively. The peak at  $1730\text{ cm}^{-1}$  in curve 1a is shifted to  $1649\text{ cm}^{-1}$  in curve 1b, revealing the involvement of C=O stretching vibration of acid derivatives, and the weak band at  $1310\text{ cm}^{-1}$  is attributed to amide groups. Curve 1b indicates the characteristic band of Fe–O at  $585\text{ cm}^{-1}$ , indicative of  $\text{Fe}_3\text{O}_4$ .

### XRD analysis

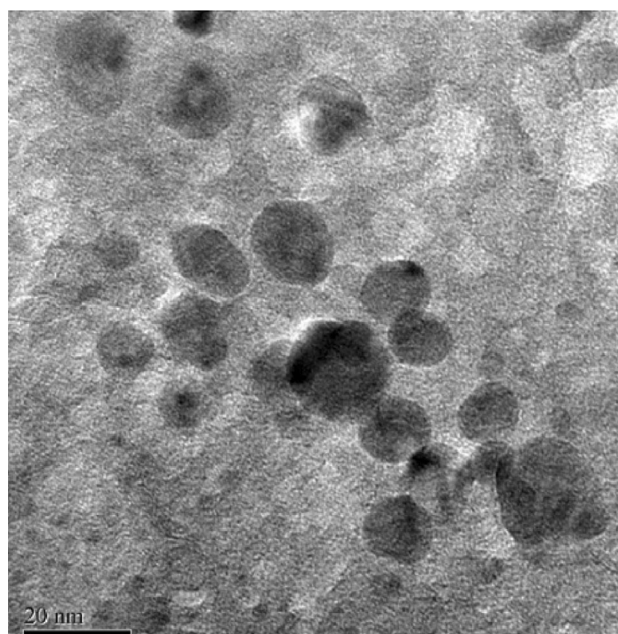
The synthesized  $\text{Fe}_3\text{O}_4$  MNPs were highly crystalline with diffraction peaks obviously assigned to the face-centered cubic phase of metallic iron. In Fig. 2, the intense diffraction peaks indexed to (220), (311), (222), (400), (422), (511) and (440) planes appearing at  $2\theta = 29.7^\circ$ ,  $35.5^\circ$ ,  $36.6^\circ$ ,  $42.6^\circ$ ,  $52.3^\circ$ ,  $57.2^\circ$  and  $62.6^\circ$ , respectively, coincide with the standard XRD data for the WR extract of iron oxide nanoparticles with a face-centered cubic structure. The crystallite size is estimated by applying the Scherres equation according to the formula,  $D = 0.89 \lambda / \beta \cos\theta$ , where  $D$  is the average particle size,  $\lambda$  is the wavelength of the Cu– $\text{K}\alpha$  irradiation,  $\beta$  is the full width at half maximum intensity of the diffraction peak and  $\theta$  is the diffraction angle for the (220) peak of iron nanoparticles. This resulted in a mean crystallite size of  $\sim 16\text{ nm}$ , which is very close to the TEM result.

### TEM and EDX analysis

TEM studies were carried out to find out the exact particle size of synthesized  $\text{Fe}_3\text{O}_4$ . Figure 3 shows the TEM image of the synthesized  $\text{Fe}_3\text{O}_4$  MNPs. The morphology and size



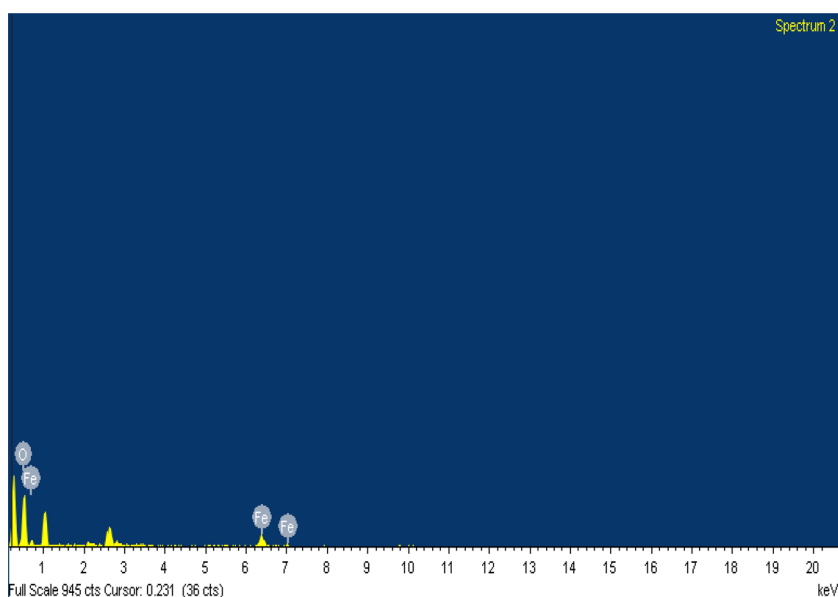
**Fig. 2** XRD pattern of  $\text{Fe}_3\text{O}_4$  MNPs synthesized using WR extract



**Fig. 3** Transmission electron microscope (TEM) image of synthesized  $\text{Fe}_3\text{O}_4$  MNPs

of the iron oxide nanoparticles are observed by TEM. Figure 3 exhibits the spherical morphology with an average size of below  $20\text{ nm}$ . The result of energy dispersive spectroscopy (EDX) analysis is shown in Fig. 4. This showed the deep-rooted significant presence of elemental iron. To confirm the whole nanocomposite which contains iron and oxygen, no additional elements were observed. The above results indicate the spherical shape and elemental iron formed by a facile manner.

**Fig. 4** Energy dispersive X-ray spectroscopy (EDS) image of synthesized  $\text{Fe}_3\text{O}_4$  MNPs



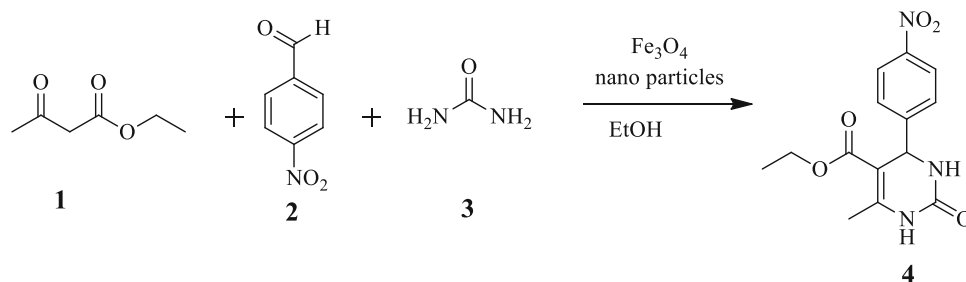
### Magnetic measurements

Figure 5 shows the hysteresis loop confirming the ferromagnetic behavior with the saturation magnetization ( $M_s$ ) value of about 14.2 emu/g, the coercive force ( $H_c$ ) of 285.58 G and magnetic remanence ( $M_r$ ) of 2.62 emu/g. The insets up left in Fig. 5 shows the behavior of magnetic nanoparticles before and after the external magnetic field. These are easily discrete in double distilled water and also could be drawn from the solution to the side wall of the vial by an external magnet. The black suspended aqueous solution turns transparent within seconds when it is placed nearby, suggesting that the obtained magnetic nanoparticles have an excellent magnetic responsive. These mag-

### Characterization data

*Ethyl 6-methyl-4-(4-nitrophenyl)-2-oxo-1,2,3,4-tetrahydropyrimidine-5-carboxylate (4)*

Yield: 82 % (pale yellow color solid); mp 253–255 °C; IR (KBr) ( $\nu_{\text{max}}/\text{cm}^{-1}$ ): 3362, 2933, 1731, 1621;  $^1\text{H}$  NMR (400 MHz;  $\text{CdCl}_2$ ):  $\delta_{\text{H}}$  1.30 (t, 3H,  $\text{CH}_3$ ), 2.41 (s, 3H,  $\text{CH}_3$ ), 4.21 (q, 2H,  $\text{CH}_2$ ), 5.62 (s, 1H, CH), 6.85 (s, 2H,  $2 \times \text{NH}$ ), 7.54 (d,  $J_{\text{HH}} = 8.0$  Hz, 2H, Ar-CH), 7.96 (d,  $J_{\text{HH}} = 8.0$  Hz, 2H, Ar-CH);  $^{13}\text{C}$  NMR (100 MHz;  $\text{DMSO}-d_6$ ):  $\delta_{\text{C}}$  20.78, 33.69, 125.58, 128.06, 135.25, 143.79, 150.64, 152.72, 154.46, 159.63, 160.79, 170.07; LC-MS (70 eV): 0  $m/z = 306$  (M+H) $^+$ .



netic properties will agree to the composites which are to be used in biomedical applications such as embattled drug delivery and also extraction of toxic metals in environment and also possessing a good recyclable property.

The prepared iron oxide nano particles have exhibited catalytic activity, so they are used for the synthesis of 2-oxo-1,2,3, 4-tetrahydropyrimidine compounds, several synthetic approaches have been devised for the synthesis of

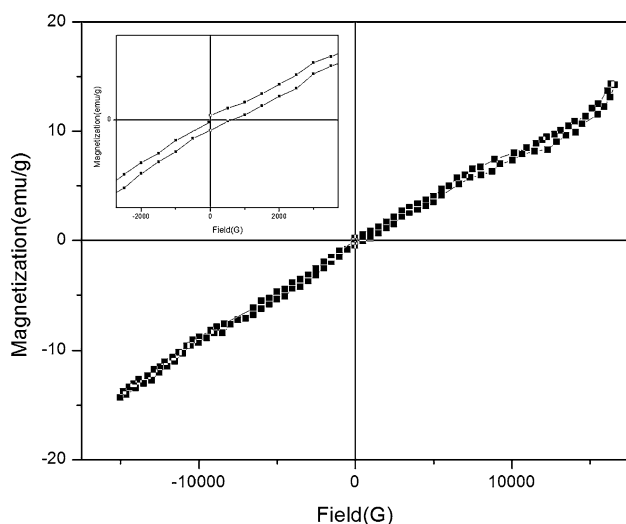


**Fig. 5** Magnetization–hysteresis (M–H) loops of  $\text{Fe}_3\text{O}_4$  MNPs measured at room temperature

tetrahydropyrimidine. To examine the catalytic ability of the synthesized  $\text{Fe}_3\text{O}_4$  nanoparticles, their catalytic efficacy for the multicomponent synthesis of ethyl 6-methyl-4-(4-nitrophenyl)-2-oxo-1,2,3,4-tetrahydropyrimidine-5-carboxylate (**4**) in ethyl alcohol as a solvent was studied. The reaction of ethylacetoacetate (1, 1.0 mmol) with nitrobenzaldehyde (2, 1.2 mmol) and urea (3, 1.2 mmol) was examined in the presence of 5 mmol of  $\text{Fe}_3\text{O}_4$  nanoparticles in ethanol solvent under reflux for 12 h, the expected cycloadduct **4** was produced in 94 % and compound **4** was determined by analysis of its spectral data. The synthesized  $\text{Fe}_3\text{O}_4$  nanoparticles-catalyzed reactions for biologically interesting oxo-1,2,3,4-tetrahydropyrimidine derivatives provided several advantages of low catalyst loading (5 mmol) and high yields (94 %).

## Conclusions

To the best of our knowledge, we have demonstrated for the first time a novel green synthesis of iron oxide nanoparticles using watermelon rind extract. The iron nanoparticles structure is confirmed by TEM result which showed that the particles were 20 nm in size with spherical shape. XRD confirmed that the iron nanoparticles have an fcc structure. Overall, the proposed green synthetic method is simple and eco-friendly, because it does not require any extra surfactants or reductants. These findings highlighted the above method for the production of excellent catalysts for use in a range of organic syntheses.

**Acknowledgments** The author Ch. Prasad acknowledges CSIR-UGC-JRF, New Delhi, India, for financial support to carry out the

present investigation. Also, the authors are thankful to IIT, Madras, and NEHU, Shillong, for providing the instrumentation facility.

**Open Access** This article is distributed under the terms of the Creative Commons Attribution 4.0 International License (<http://creativecommons.org/licenses/by/4.0/>), which permits unrestricted use, distribution, and reproduction in any medium, provided you give appropriate credit to the original author(s) and the source, provide a link to the Creative Commons license, and indicate if changes were made.

## References

- Cai Y, Shen Y, Xie A, Li S, Wang X (2010) Green synthesis of soya bean sprouts-mediated superparamagnetic  $\text{Fe}_3\text{O}_4$  nanoparticles. *J Magn Magn Mater* 322:2938
- Chen Y, Chen H, Zeng D, Tian Y, Chen F, Feng J, Shi J (2010) Core/shell structured hollow mesoporous nanocapsules: a potential platform for simultaneous cell imaging and anticancer drug delivery. *ACS Nano* 4:6001
- Chen W, Yi P, Zhang Y, Zhang L, Deng Z, Zhang Z (2011) Interfaces. Composites of aminodextran-coated  $\text{Fe}_3\text{O}_4$  nanoparticles and graphene oxide for cellular magnetic resonance imaging. *ACS Appl Mater* 3:4085
- Cheng Q, Qu F, Li NB, Luo HQ (2012) Mixed hemimicelles solid-phase extraction of chlorophenols in environmental water samples with 1-hexadecyl-3-methylimidazolium bromide-coated  $\text{Fe}_3\text{O}_4$  magnetic nanoparticles with high-performance liquid chromatographic analysis. *Anal Chim Acta* 715:113
- Deng Y, Wang L, Yang W, Fu S, Elaissari A (2003) Preparation of magnetic polymeric particles via inverse microemulsion polymerization process. *J Magn Magn Mater* 257:69
- Durmus Z, Kavas H, Toprak MS, Baykal A, Altuncelik TG, Aslan A, Bozkurt A, Cosgun S (2009) L-lysine coated iron oxide nanoparticles: synthesis, structural and conductivity characterization. *J Alloys Compd* 484:371
- Franger S, Berthet P, Berthon J (2004) Electrochemical synthesis of  $\text{Fe}_3\text{O}_4$  nanoparticles in alkaline aqueous solutions containing complexing agents. *J Solid State Electrochem* 8:218
- Gupta AK, Gupta M (2005) Synthesis and surface engineering of iron oxide nanoparticles for biomedical applications. *Biomaterials* 26:3995
- Hayakawa H, Tanaka H, Fujimoto K (2007) Preparation of a new precipitated iron catalyst for Fischer-Tropsch synthesis. *Catal Commun* 8:1820
- He X, Wu X, Xin CAI, Lin S, Xie M, Zhu X, Yan D (2012) Functionalization of magnetic nanoparticles with Dendritic–Linear–Brush-like triblock copolymers and their drug release properties. *Langmuir* 28:11929
- Hornbaker DJ, Kahng SJ, Misra S, Smith BW, Johnson AT, Mele EJ, Luzzi DE, Yazdani A (2002) Mapping the one-dimensional electronic states of nanotube peapod structures. *Science* 295:828
- Hua J, HeQing Y (2008) Controlled synthesis and magnetic properties of  $\text{Fe}_3\text{O}_4$  walnut spherical particles and octahedral microcrystals. *Sci China Tech Sci* 51:1911
- Jabera J, Mohsen E (2013) Synthesis of  $\text{Fe}_3\text{O}_4$  silica/poly(*N*-isopropylacrylamide) as a novel thermo-responsive system for controlled release of  $\text{H}_3\text{PMO}_{12}\text{O}_{40}$  nano drug in AC magnetic field. *Colloids Surf B* 102:265
- Lakshmiathy R, Vinod AV (2013) Watermelon rind as biosorbent for removal of  $\text{Cd}^{2+}$  from aqueous solution: FTIR, EDX and kinetic studies. *J Indian Chem Soc* 90:1147

- Li X, Yan XY (2012) Suzuki-Miyaura cross-couplings of arenediazonium tetrafluoroborate salts with arylboronic acids catalyzed by aluminium hydroxide-supported palladium nanoparticles. *Org Biomol Chem* 10:495
- Lu AH, Schmidt W (2004) Nanoengineering of a magnetically separable hydrogenation catalyst. *Angew Chem Int Ed* 43:4303
- Lu W, Yuhua Shen, Anjian Xie, Weiqiang Zhang (2010) Green synthesis and characterization of superparamagnetic Fe<sub>3</sub>O<sub>4</sub> nanoparticles. *J Magn Magn Mater* 322:1828
- Narayanan KB, Sakthivel N (2011) Extracellular synthesis of silver nanoparticles using the leaf extract of *Coleus amboinicus* Lour. *Mater Res Bull* 46:1708
- Nazrul Islam MD, VanPhong L, Jeong JR, Kim CG (2011) A facile route to sonochemical synthesis of magnetic iron oxide (Fe<sub>3</sub>O<sub>4</sub>) nanoparticles. *Thin Solid Films* 519:8277
- Sanchez ML, Primo A, Garcia H (2012) Green synthesis of Fe<sub>3</sub>O<sub>4</sub> nanoparticles embedded in a porous carbon matrix and its use as anode material in Li-ion batteries. *J Mater Chem* 22:21373
- Sun C, Lee JSH, Zhang M (2008) Magnetic nanoparticles in MR imaging and drug delivery. *Adv Drug Deliv Rev* 60:1252
- Venkateswarlu S, SubbaRao Y, Balaji T, Prathima B, Jyothi VVN (2013) Biogenic synthesis of Fe<sub>3</sub>O<sub>4</sub> magnetic nanoparticles using plantain peel extract. *Mater Lett* 100:241
- Wang J, Wu YJ, Zhu Y (2007) Fabrication of complex of Fe<sub>3</sub>O<sub>4</sub> nanorods by magnetic-field-assisted solvothermal process. *J Mater Chem Phys* 106:1
- Wang Z, Zhu H, Wang X, Yang F, Yang X (2009) One-pot green synthesis of biocompatible arginine-stabilized magnetic nanoparticles. *Nanotechnology* 20:465
- Wu JH, KoS P, Liu HL, Jung MH, Lee JH, SeonJU J, Kim YK (2008) Sub 5 nm Fe<sub>3</sub>O<sub>4</sub> nanocrystals via coprecipitation method. *Colloids Surf A Physicochem Eng Aspects* 313:268
- Zhang N, Peng H, Hu BIN (2012) Light-induced pH change and its application to solid phase extraction of trace heavy metals by high-magnetization Fe<sub>3</sub>O<sub>4</sub>@SiO<sub>2</sub>@TiO<sub>2</sub> nanoparticles followed by inductively coupled plasma mass spectrometry detection. *Talanta* 94:278
- Zhou L, Xu J, Miao H, Wang F, Li X (2005) Catalytic oxidation of cyclohexane to cyclohexanol and cyclohexanone over Co<sub>3</sub>O<sub>4</sub> - nanocrystals with molecular oxygen. *Appl Catal A* 292:223
- Zou GF, Xiong K, Jiang CG, Li H, Li TW, Du J, Qian YT (2005) Fe<sub>3</sub>O<sub>4</sub> nanocrystals with novel fractal. *J Phys Chem B* 109:18356